



## Research paper

# Combined engine configuration and speed optimization for fuel savings on cruise ships

Arash Marashian<sup>a</sup>, Jari M. Böling<sup>b,a</sup><sup>\*</sup>, Abolhassan Razminia<sup>a,c</sup>, Jari Hyvönen<sup>d</sup>, Roberto Vettor<sup>e</sup>, Wilhelm Gustafsson<sup>f</sup>, Mathias Pirttikangas<sup>f</sup>, Jerker Björkqvist<sup>g</sup>

<sup>a</sup> Process and Systems Engineering, Faculty of Science and Engineering, Åbo Akademi University, Turku, Finland

<sup>b</sup> Department of Mechanical and Materials Engineering, University of Turku, Finland

<sup>c</sup> Department of Electrical Engineering, Persian Gulf University, Bushehr, Iran

<sup>d</sup> Wärtsilä Ltd, Vaasa, Finland

<sup>e</sup> Napa Ltd, Helsinki, Finland

<sup>f</sup> Meyer Turku Ltd, Turku, Finland

<sup>g</sup> Information Technology, Faculty of Science and Engineering, Åbo Akademi University, Turku, Finland

## ARTICLE INFO

## Keywords:

Engine configuration  
Fuel efficiency  
Speed optimization  
Data-driven modeling  
Cruise ship

## ABSTRACT

In the maritime industry, optimizing energy systems for cruise ships is critical for enhancing fuel efficiency and advancing sustainability. This study presents a novel approach that integrates empirical data and computational modeling techniques with a combination of optimization of the engine configuration and the speed of the ship. A methodology aimed at minimizing fuel consumption while keeping timetable is developed using dynamic programming. The presented approach uses the NAPA Voyage Optimization API to provide information about how the ship requires propulsion power for keeping a certain speed at the weather conditions at hand. Passenger-induced hotel load and other non-propulsion auxiliary load are predicted using a machine learning model obtained from ship data. The proposed method shows in a test case fuel savings of up to 3.3% with conventional engines and 2.7% with next-generation engines. Furthermore, optimizing the sizes of engines contribute to an additional 0.5% reduction in the fuel consumption.

## 1. Introduction

In 2018, emissions from worldwide shipping contributed to approximately 2.9% of the total global emissions attributed to human activities (European, 2024). In July 2023, the International Maritime Organization (IMO) committed to new GHG emissions reduction targets and aims to develop and adopt a set of measures by 2025 to meet these targets (IMO, 2024). Additionally, the EU's actions to ensure that maritime transport contributes to achieving climate neutrality in Europe by 2050 are essential for incentivizing the necessary reductions (IMO, 2024).

The cruise ship industry has seen a steady rise in the number of yearly passengers, with an exception in recent years due to the global pandemic, which will make it even more challenging to meet the reduction targets. Cruise line companies will have increased incentives to reduce emissions and fuel consumption to attract customers who are increasingly aware of the industry's environmental impact (Piispa,

2020). The industry has to explore new fuel options and ways to reduce overall fuel consumption in order to achieve the goals set by the IMO. Several studies have been done to take a step in the decarbonization and sustainability direction (Bouman et al., 2017). Some of them are improving the power and propulsion systems (Tillig et al., 2015), using alternative fuels (Kim et al., 2020) and energy sources (Balsamo et al., 2020), developing efficient hulls (Tadros et al., 2023), and optimizing the operational aspects (van Dooren et al., 2023).

By suggesting an optimized ship speed profile along a given route to force the engines to work at their optimal load level, optimal fuel consumption and, thus, the CO<sub>2</sub> emissions reduction can be experienced. To do so, firstly, the power demand of the system should be well predicted. The power demands of cruise ships consist of three main parts: propulsion, hotel, and auxiliary. The propulsion system is highly dependent on the ship's speed and environmental conditions. The hotel system is dependent on environmental variables and passenger

\* Corresponding author at: Department of Mechanical and Materials Engineering, University of Turku, Finland.

E-mail addresses: [seyedarash.marashian@abo.fi](mailto:seyedarash.marashian@abo.fi) (A. Marashian), [jari.boling@utu.fi](mailto:jari.boling@utu.fi) (J.M. Böling), [abolhassan.razminia@abo.fi](mailto:abolhassan.razminia@abo.fi) (A. Razminia), [jari.hyvonen@wartsila.com](mailto:jari.hyvonen@wartsila.com) (J. Hyvönen), [roberto.vettor@napa.fi](mailto:roberto.vettor@napa.fi) (R. Vettor), [wilhelm.gustafsson@meyerturku.fi](mailto:wilhelm.gustafsson@meyerturku.fi) (W. Gustafsson), [mathias.pirttikangas@meyerturku.fi](mailto:mathias.pirttikangas@meyerturku.fi) (M. Pirttikangas), [jerker.bjorkqvist@abo.fi](mailto:jerker.bjorkqvist@abo.fi) (J. Björkqvist).

<https://doi.org/10.1016/j.oceaneng.2025.120387>

Received 29 July 2024; Received in revised form 7 January 2025; Accepted 12 January 2025

Available online 27 January 2025

0029-8018/© 2025 The Authors. Published by Elsevier Ltd. This is an open access article under the CC BY license (<http://creativecommons.org/licenses/by/4.0/>).

activities, and the auxiliary system mainly depends on the propulsion power.

The number of papers published in ship weather routing and voyage optimization has steeply increased in recent years, from less than ten papers per year before 2004 to around 50 per year after 2014 (Zis et al., 2020). Most articles on voyage optimization are for cargo ships. For example, Psaraftis and Kontovas (2014) explores concepts and modeling approaches for ship speed optimization and routing scenarios, but cruise ships or hotel load is not discussed. Radonja et al. (2019) do cruise ship speed optimization, but varying weather conditions and hotel load are not considered. A central part of voyage optimization is to predict the energy flows, and fuel consumption prediction is reviewed in Fan et al. (2022). A study that analyzed the energy and exergy flow rates of a cruise ship sailing in the Baltic Sea found that the power demand follows repeatable trends over time (Baldi et al., 2018).

Compared to cargo ships, a considerable part of the power consumption on cruise ships comes from the hotel load. Much of the existing research focuses on propulsion systems, with fewer studies addressing cruise ships' unique energy demands. It is reported in Brækken (2021) that hotel systems account for up to 40% of a cruise ship's total energy consumption, especially in challenging climates such as the Nordic region. They explored various energy-saving measures, including passive and active methods, to reduce energy use, highlighting the significant impact of heat pumps and improved ventilation systems on reducing hotel load power demand. Another research proposed a hybrid approach combining constraint-based algorithms and Gaussian Process Regression (GPR) for estimating hotel load power demands (Micallef et al., 2024). Their study highlighted the importance of accurately predicting hotel loads for optimizing auxiliary engine performance, with sensitivity analysis revealing the strong influence of ship parameters such as gross tonnage and engine power on hotel power consumption. Furthermore, Simonsen et al. developed a model in Simonsen et al. (2018) for estimating cruise ships' fuel consumption in Norwegian waters. Their model uses Automatic Identification System (AIS) data and technical ship information such as service speed, total power, and the number of engines. This study highlights the importance of considering propulsion and hotel loads in the fuel consumption model for cruise ships.

Cruise ships, especially newer ones, usually use a diesel–electric propulsion system (Hansen and Wendt, 2015). All engines generate electrical power that can be used for propulsion or any of the other systems on the ship. This introduces flexibility in the production of energy, which can be utilized to schedule the production so that the energy is produced at the best possible efficiency. Conventional marine diesel engines typically have their best efficiency at 80%–85% load level (Wärtsilä, 2024). On the other hand, next-generation engines, which can run based on gas, Light Fuel Oil (LFO), or Liquid BioFuel (LBF), have an optimal efficiency at 100% load. These engines have high power-to-weight and power-to-space ratios and can meet the IMO Tier III regulations.

Empirical data is used to model the hotel and auxiliary systems aboard cruise ships to predict these energy sinks. The NAPA Voyage Optimization APIs (NAPA, 2023), is used for prediction of the required propulsion power as function of ship speed and predicted weather conditions.

System modeling can be accomplished through several techniques, including regression-based expected behavior models (Cheliotis et al., 2020), ensemble learning models (Li et al., 2021), extreme learning machine and neural network (Fang et al., 2019), and linear-parameter-varying (LPV) modeling (Marashian et al., 2024a). Furthermore, speed profile control can be achieved through various methods: Optimal Control (Psaraftis and Kontovas, 2014), adaptive control (Simorgh et al., 2024, 2019), and Dijkstra's algorithm (Huotari et al., 2021; Ma et al., 2020; Marashian and Razminia, 2024).

**Table 1**  
Terminology and abbreviations.

Abbreviation term	Description	Abbreviation term	Description
SFC	Specific fuel consumption	API	Application programming interface
NCA	Neighborhood component analysis	ANN	Artificial neural networks
LS	Least squares	HVAC	Heating, ventilation, and air conditioning
GA	Genetic Algorithm	LFO	Light Fuel Oil
LBF	Liquid BioFuel	MDO	Marine Diesel Oil
MGO	Marine Gas Oil	IMO	International maritime organization
MSE	Mean Squared Error	AIS	Automatic identification system

In this paper, two slightly different problems are presented and solved. First, the total fuel consumption is minimized by changing the ship speed, which was first presented in Marashian et al. (2024b). For the speed optimization, predictions of the total fuel consumption is utilized. Main novelty in this step is the use of the efficiency curve of the used engines. Furthermore, the optimal choice of engine sizes is studied, utilizing the speed optimization as a subproblem after a certain choice of engines. Furthermore, both conventional and next-generation engines are studied separately. The speed optimization is done using dynamic programming, and the engine size optimization is performed a genetic algorithm, an optimization approach that provides near-optimal solutions by exploring multiple possibilities, often used when finding an exact solution is computationally expensive or impractical.

The remainder of this paper is structured as follows: in the next section, the data is prepared, and the necessary models are developed. In Section 3, the speed profile optimization problem is formulated and solved in different scenarios. After that, the algorithm developed in Section 4 is used to find the best engine sizes for the studied cruise ship. At the end, in Section 5, conclusions and potential directions for future research are given. A table summarizing the key terminology and abbreviations can be found in Table 1 for quick reference.

## 2. Hotel and auxiliary load modeling

A key feature used in this paper is the engine load-dependent Specific Fuel Consumption (SFC) curve of the studied engines, including taking into account that the curve depends on the number of engines on. The total fuel consumption is calculated based on the total power consumption using the SFC curve. In this paper, the power consumption on the ship is categorized into three parts as

$$P_{total}(t) = P_{prop}(t) + P_{aux}(t) + P_{hotel}(t), \quad (1)$$

where  $P_{prop}$  is the power usage of the propulsors,  $P_{aux}$  is the power demand of the auxiliary part of the cruise ship, and finally,  $P_{hotel}$  is the power consumption of the hotel. Propulsion includes the two main propulsors and the maneuvering thrusters, and it can be calculated based on a certain choice of ship speed using the NAPA Voyage Optimization tool.

Hotel power is defined as everything which depends on passenger activities and comfort, for example HVAC. Auxiliary power encompasses all other factors, that are mostly related to the engines, for example pumping of cooling water. Auxiliary power is influenced by the hotel load and the propulsion, but not the other way around.

The propulsion power is predicted via NAPA Voyage Optimization APIs (NAPA, 2023). The required power is estimated using a comprehensive hydrodynamic model that considers the combined effects of wind, waves, swell, current, shallow water, and rudder angle to

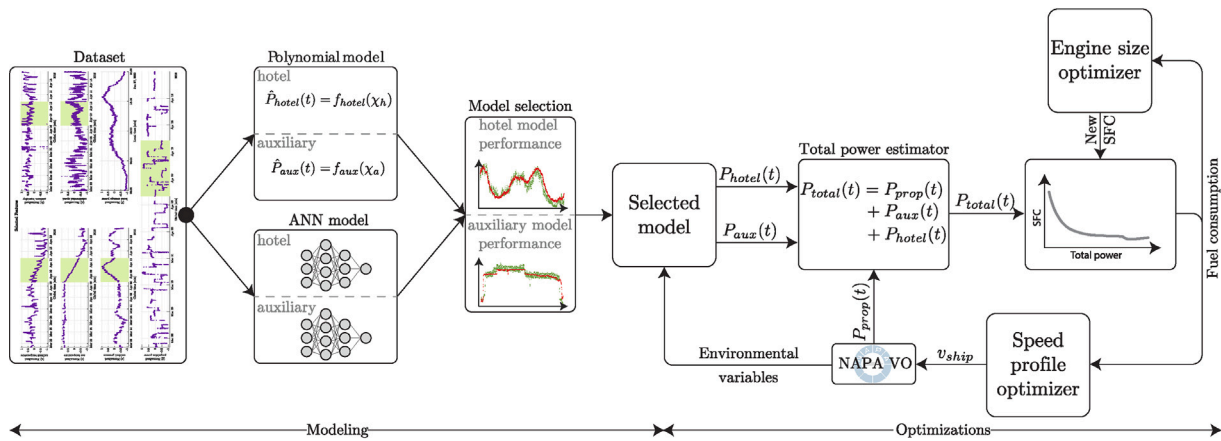


Fig. 1. Overview of the proposed procedure in this study. The first step is modeling, the second step is speed optimization, and the third step is engine size optimization (under which step two is included).

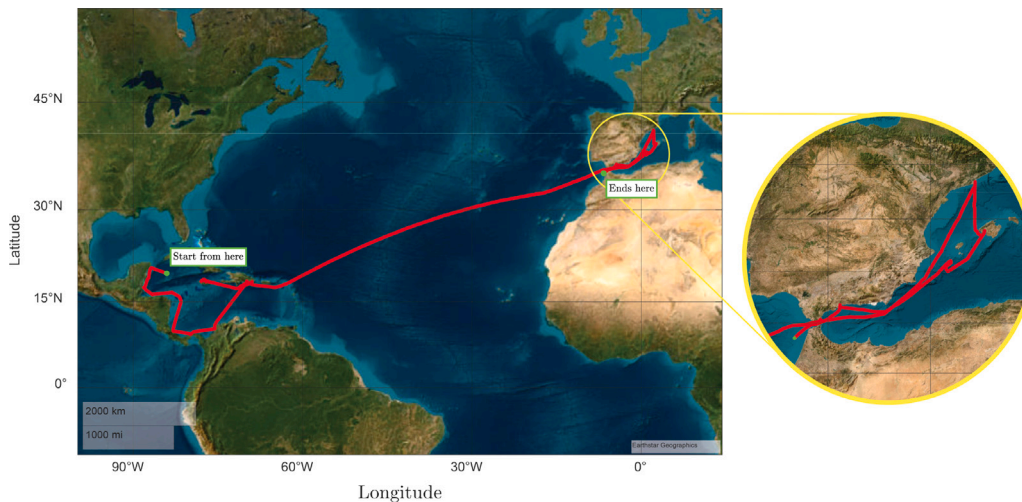


Fig. 2. Route taken by the case ship during one month.

calculate hull resistance under forecasted weather conditions. NAPA also compare predictions to operational data, and refine the predictions with a number of tuning parameters. In the optimization model utilized in this research, the speed, time, and coordinates of a particular ship are inputted into the NAPA API, and the corresponding propulsion power is received as output. The NAPA API acquires the hydro-meteorological condition predictions from Tidetech (Tidetech, 2024). This means that the hotel and auxiliary power consumption models are the only ones that are needed for this study. All steps considered in this work, including the speed and engine-size optimization, are illustrated in Fig. 1.

In Marashian et al. (2024b), two alternative methods were investigated to model the hotel and auxiliary power system. In this paper, the one that was found to perform better, an Artificial Neural Network (ANN) is used.

Data from a mid-sized cruise ship primarily operating in the Caribbean and Mediterranean Seas has been comprehensively analyzed in this study, see Fig. 2 for the route taken by the ship, with specifications and characteristics provided as follows. The tonnage is 100,000 gross tons and dimensions of 295 m in length and 42 m in beam. The considered ship was constructed in 2017, and possesses a conventional diesel–electric propulsion system, and has a total installed power capacity of 48 MW.

Power consumption distribution across different ship systems varies in maritime operations depending on the ship’s operational state. In

the two predominant operational states, the allocation of power varies significantly: During the sailing phase, propulsion systems consume 69% of the total power, hotel services account for 13%, and auxiliary systems utilize the remaining 18%. Conversely, when the vessel is docked at the harbor, the power distribution shifts dramatically, with only 6% allocated to propulsion, 52% to hotel services, and 42% to auxiliary systems. It should be noted that speed optimization is not a concern during the harboring state, rendering this particular operational condition outside the scope of the present research.

The data in this study has been categorized as the following datasets (see Fig. 3):

1. **Port:** using the ship speed-over-ground feature, the data related to the time that the ship has stopped at the harbor is omitted from the dataset, as the focus of the paper is on optimizing the speed of the ship in the first place.
2. **Atlantic crossing:** this voyage spanned from 06 April at 23:29 to 13 April at 05:20. This data is important as the environmental characteristics will change more during this crossing.
3. **Training:** about half of the voyage data will serve as the training set. This dataset will be used entirely to generate the model.
4. **Validation:** part of the remaining data will be used for validation. This division is designed to ensure that the validation performance closely reflects the actual performance of the model.

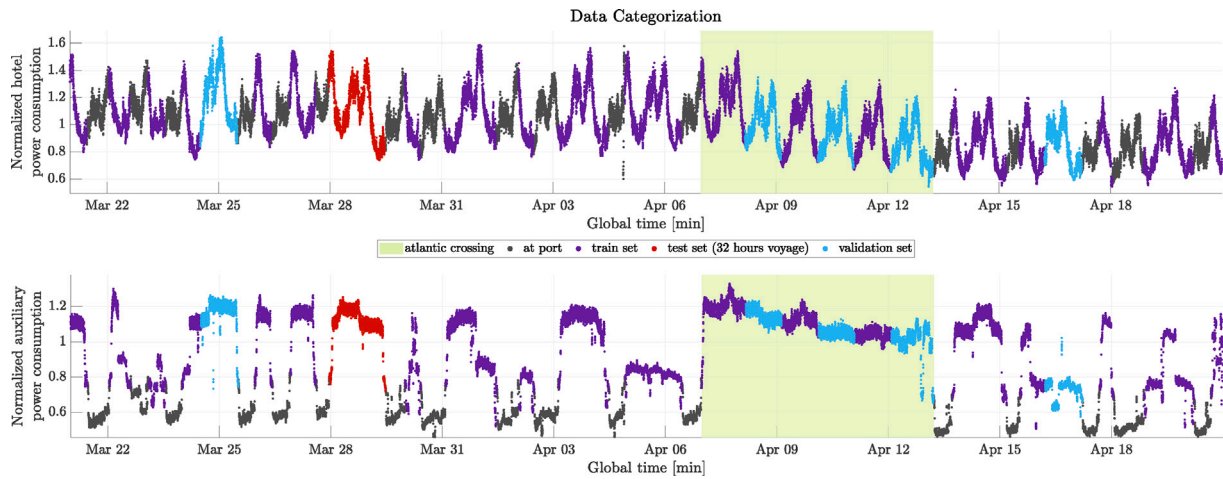


Fig. 3. The one-month data is divided into four different categories.

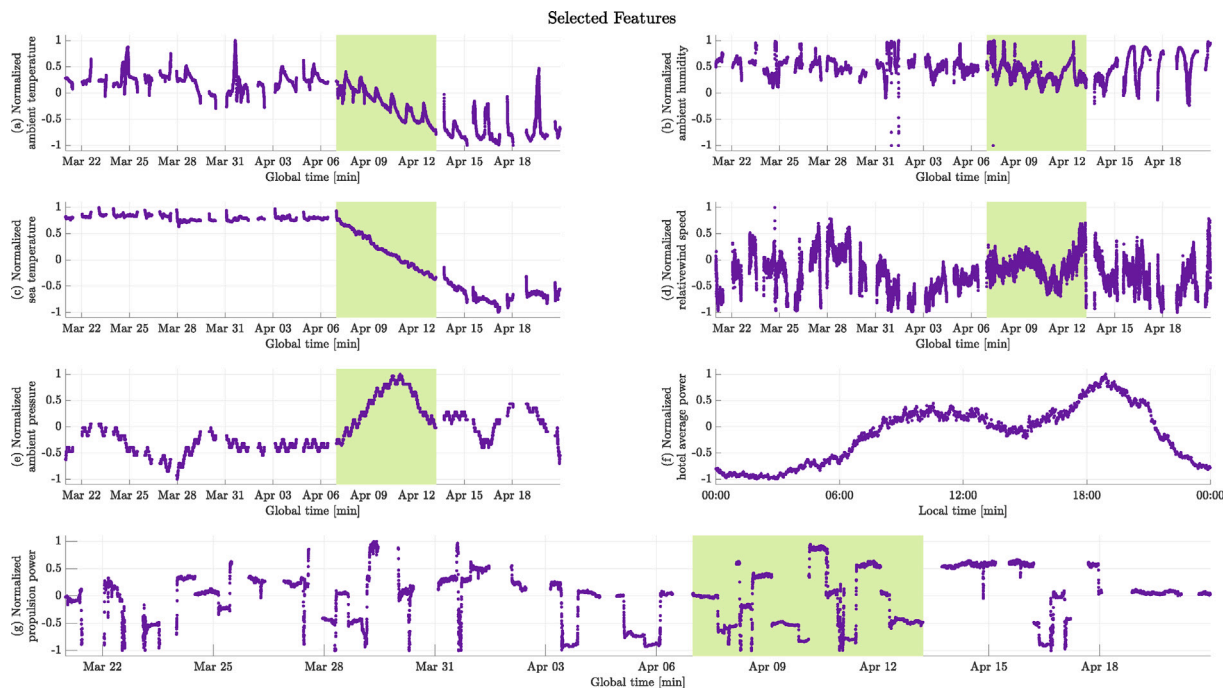


Fig. 4. Selected normalized features based on the Neighborhood Component Analysis. It can be seen that the weather characteristics changed substantially after the Atlantic crossing voyage.

- 5. **Test:** a 32-h voyage has been considered as a test dataset. This dataset evaluates the model's performance on unseen data, testing its generalization ability.

2.1. Data assessment

For this study, one month of operational data is used. The features considered for the prediction of the power signals are all the available environmental variables, the number of passengers, the number of passengers, and three power signals, closer described next.

Hotel load is defined as all the power consumption that is related to passengers. The passengers are served meals at a certain time of day, and this makes the hotel load quite strongly dependent on the time of the day. This is useful for prediction of hotel load, and for this purpose a feature consisting of the hourly average hotel load, denoted ( $P_{hotel,avg}$ ). Fig. 4(f) depicts normalized hotel average power.

For prediction of the auxiliary load, consisting of power consumption related to the engines, one can more feature is considered. The

auxiliary load is correlated to the total load, and a prediction of the propulsion power is available after a certain choice of ship speed. Thus it can be used for prediction of auxiliary load. The hotel load again effects the propulsion load in the data, through operator decisions, and one should thus not use it for prediction of the hotel load, as such operator decisions are made at a later time, not at the time of prediction.

For the selection of the relevant features in Table 2 a tool called Neighborhood Component Analysis (NCA) (Yang et al., 2012) was utilized. NCA is a nonlinear, non-parametric feature selection technique designed for regression tasks. This method assigns weights to each feature based on their importance for modeling, with higher weights implying more important feature. The NCA weights for the considered features for each prediction task is presented in Table 2. The model is constructed such that the features are forward selected in the order determined by their corresponding NCA weights. Each selection of feature is tested using the performance of the obtained model on validation data. If no improvement is obtained compared with the model without the selected feature, the feature is removed, and the selection process

**Table 2**  
Key features and their significance in hotel and auxiliary power modeling.

Features	(notation)	Hotel	Feature wight	Auxiliary	Feature wight
Ambient temperature	$(\mathcal{T}_{amb})$	√	8.613	√	7.793
Relative ambient humidity	$(\mathcal{H}_{amb})$	√	8.291	×	6.214
Number of passengers	$(\mathcal{N}_{psg})$	×	1.315	×	0.432
Sea temperature	$(\mathcal{T}_{sea})$	√	4.969	√	7.587
Relative wind speed	$(\mathcal{V}_{wind})$	√	5.433	×	3.156
Ambient pressure	$(\mathcal{P}_{amb})$	√	5.35	×	4.609
Moist air enthalpy	$(\mathcal{H}_m)$	×	0.007	×	3.503
Hotel average power	$(\mathcal{P}_{hotel,avg})$	√	7.412	×	0.011
Propulsion power	$(\mathcal{P}_{prop})$	×	–	√	6.408

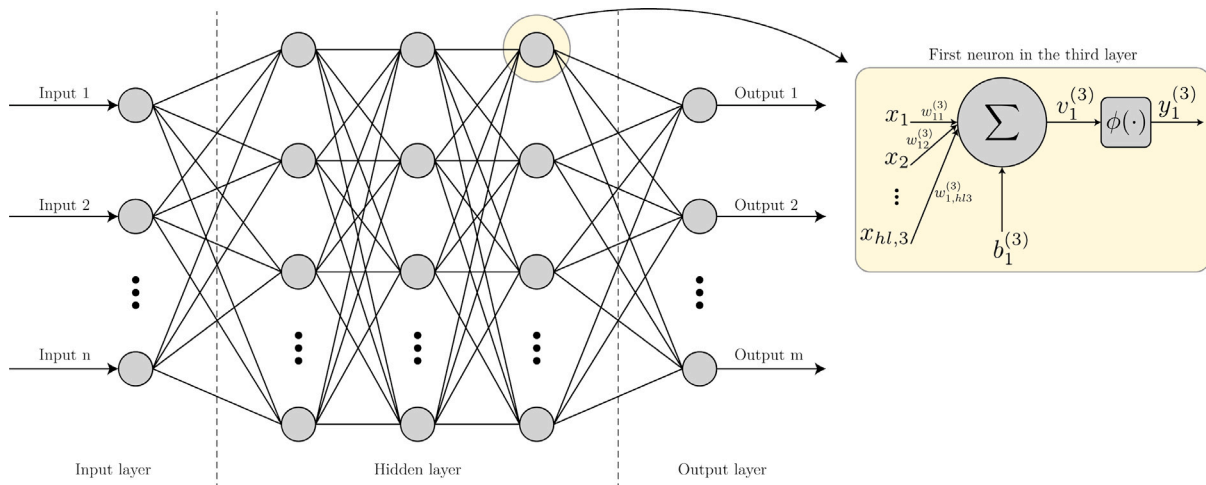


**Fig. 5.** Neural network standard structure.

**Table 3**  
Backward elimination to verify the importance of the selected features.

System	Eliminated feature	Train MSE	Test MSE
Hotel	(none)	0.0232	0.0220
	$\mathcal{T}_{amb}$	0.0198	0.0457
	$\mathcal{H}_{amb}$	0.0209	0.0422
	$\mathcal{T}_{sea}$	0.0198	0.0353
	$\mathcal{V}_{wind}$	0.0301	0.0390
	$\mathcal{P}_{amb}$	0.0588	0.0905
	$\mathcal{P}_{hotel,avg}$	0.0949	0.1717
	All features+ $\mathcal{N}_{psg}$	0.0364	0.0313
	Auxiliary	(none)	0.0490
$\mathcal{T}_{amb}$		0.0560	0.0344
$\mathcal{T}_{sea}$		0.0490	0.0367
$\mathcal{P}_{prop}$		0.1411	0.1090

stops.

The results of the above described selection process is presented in Table 2, described in Section 2.2. A bit surprisingly the number of passengers did not affect the hotel load. This is most likely due to that the number does not vary enough in the considered data set, the ship is most of the time quite full.

The selected features were furthermore tested using backward elimination of one selected feature at a time, which is presented in Table 3. This test revealed that the NCA process seemed to be quite accurate for selection of features for the ANN model. Additionally, adding the number of passengers feature was also tested, which is also presented in Table 3. The performance of both models on validation data were reduced, and thus the number of passengers were not used.

## 2.2. Artificial neural network model

Artificial Neural Networks (ANN) are computational models inspired by the structure and function of the human brain. They consist of interconnected nodes, called neurons, organized in layers. The layers typically include an input layer, one or more hidden layers, and an output layer. Fig. 5 depicts a general ANN model with  $n$  number of inputs, three hidden layers, and  $m$  number of outputs. Consider the  $k$ th neuron in the  $j$ th hidden layer, its output is calculated as

$$y_k^{(j)} = \phi \left( \sum_{i=1}^{hl_j} x_i w_{ki}^{(j)} + b_k^{(j)} \right) \quad (2)$$

where  $x_i$  is the output of the previous layer,  $w_{i,j}$  is the weight between neuron  $k$  in the  $j$ th layer and neuron  $i$  in the  $(j-1)$ th layer,  $b$  is the bias of the neuron, and  $\phi(\cdot)$  is the activation function. There are several standard activation functions, like the Sigmoid Function which is  $\phi_{\text{sigmoid}}(x) = (1 + e^{-x})^{-1}$ , ReLU which is  $\phi_{\text{ReLU}}(x) = \max(0, x)$ , and tansig which is  $\phi_{\text{tansig}}(x) = 2(1 + e^{-2x})^{-1} - 1$ . Here, the tansig activation function was used for the hidden layers. The Purelin activation function  $\phi(x) = x$  is used in the output layer.

The weights and biases, that is,  $w_{ij}^{(k)}$  and  $b_i^{(k)}$ , are the network parameters which are commonly optimized using backpropagation. This process involves computing the gradients of the loss function concerning the network parameters and updating them using gradient descent, stochastic gradient descent, or the Levenberg–Marquardt algorithm (which is used in this paper).

An ANN's number of layers and neurons significantly affects its performance and pattern-learning capabilities. Employing a grid search method, various architectures were systematically tested to find optimal structures. For the hotel model, which is denoted by  $\mathcal{N}_{hotel}(\mathcal{T}_{amb}, \mathcal{H}_{amb}, \mathcal{T}_{sea}, \mathcal{V}_{wind}, \mathcal{P}_{amb}, \mathcal{P}_{hotel,avg})$ , one hidden layer with 11 neurons was determined to be optimal. In contrast, for the auxiliary model, which is denoted by  $\mathcal{N}_{aux}(\mathcal{T}_{amb}, \mathcal{T}_{sea}, \mathcal{P}_{prop})$ , three hidden layers with 15, 3, and 3

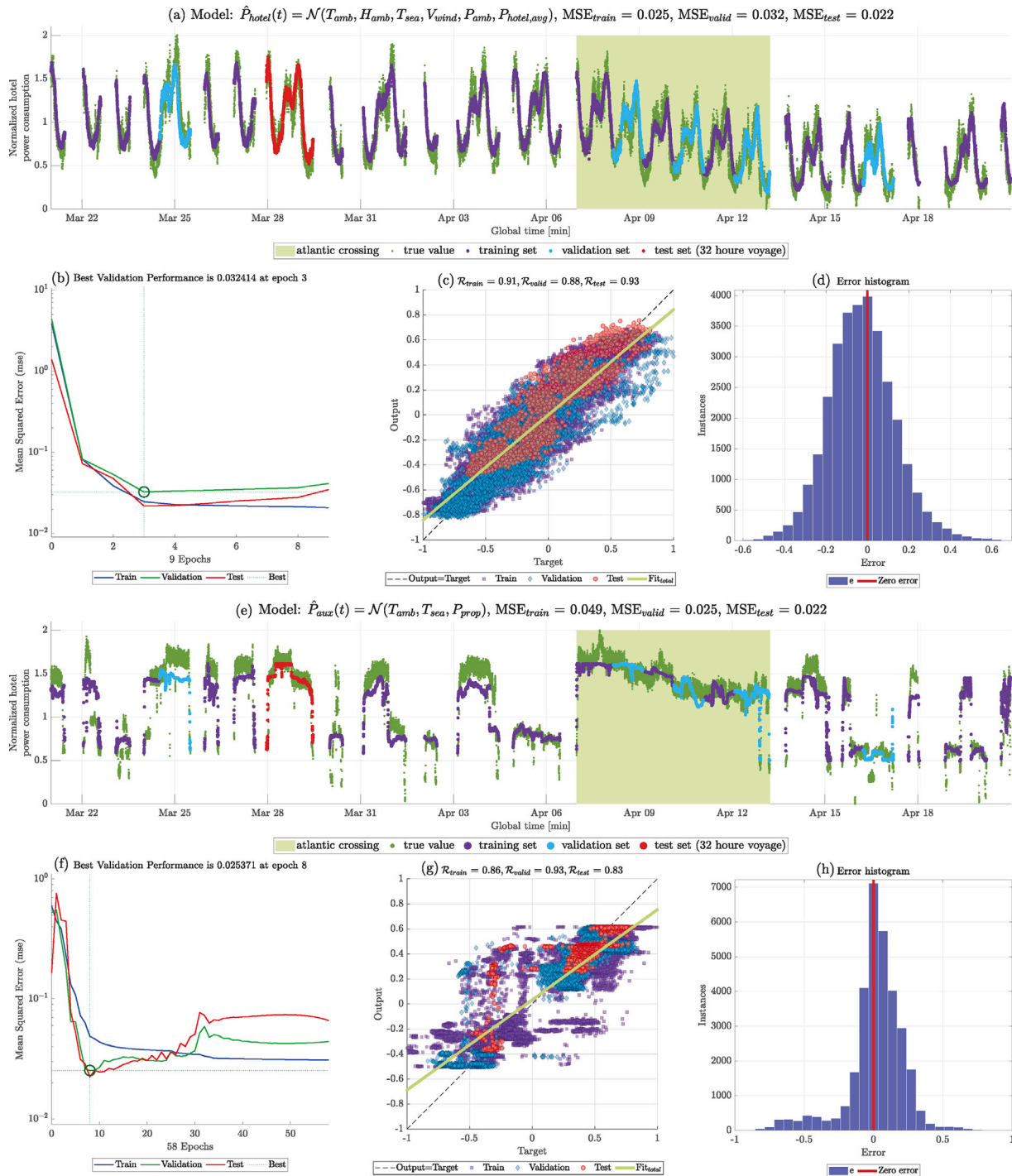


Fig. 6. Neural network model response for both hotel and auxiliary power systems. The error histogram is on all datasets, i.e., training, validation, and test.

neurons in each layer respectively were found to be optimal.

Table 3 highlights features’ significance in hotel and auxiliary system modeling. The hotel’s average power emerges as the most crucial feature for the hotel models. For the model predicting the auxiliary power propulsion power is the most important feature.

The results of the neural network can be seen in Fig. 6. The details are discussed below.

**Hotel model performance:** Considering Fig. 6-(a), the model exhibits robust and smooth behavior, effectively tracking trend changes post-Atlantic crossing. MSE values for the training, validation, and test datasets are 0.025, 0.032, and 0.022, respectively. In Fig. 6-(b), the

optimizer achieves peak performance after three epochs, indicating potential for efficient online learning in future research. The  $\mathcal{R}$  factors for the same datasets are 0.91, 0.88, and 0.93, respectively, indicating a strong correlation between model output and actual values. The histogram in Fig. 6-(d) suggests the model is unbiased.

**Auxiliary model performance:** Considering the complexity of the auxiliary system, the model’s performance in Fig. 6-(e) is acceptable, with MSE values for training, validation, and test datasets at 0.049, 0.025, and 0.022, respectively. The optimizer reaches the best model after eight epochs.  $\mathcal{R}$  factors for the same datasets are 0.86, 0.93, and 0.83, respectively. The histogram plot in Fig. 6-(h) indicates minimal bias,

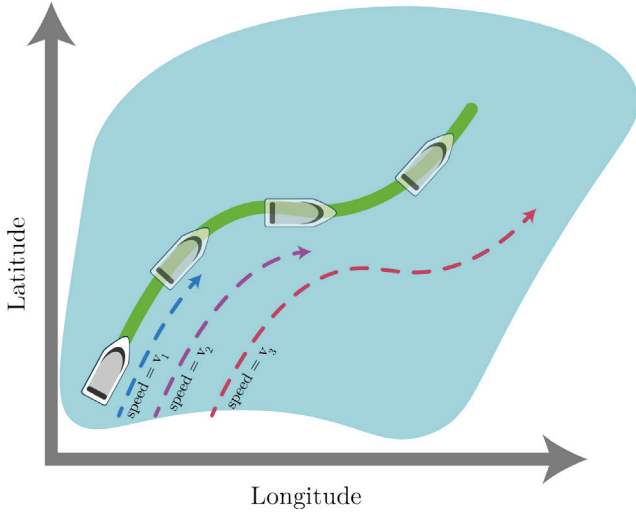


Fig. 7. Effect of choosing different speeds on cruise ship's position at next time step.

although occasional overestimation is observed.

### 3. Speed optimization

The ship's speed significantly impacts fuel consumption, which is determined by engine power and auxiliary system demands. Here, an algorithm is proposed to optimize cruise ship speed, factoring in hotel load, auxiliary, and propulsion systems to minimize fuel consumption.

Different speed profiles affect the ship's location (Fig. 7). As models rely on environmental variables, the problem is discretized in time using hourly steps, and the variables are obtained from NAPA Voyage Optimization API. With these variables, hotel ( $P_{hotel}$ ) and auxiliary ( $P_{aux}$ ) power demands can be predicted using the ANN model described in the previous section. Propulsion power ( $P_{prop}$ ) for each speed will be estimated via the NAPA API. This process generates a graph from start to goal points, with edges determining fuel consumption.

Considering the ship's speed at step  $q$  being  $v_q \in \mathcal{V} = \{v_1, v_2, \dots, v_N\}$ , and the grid points being  $p \in \mathcal{P} = \{p_0, p_1, \dots, p_N\}$  as it is shown in Fig. 8, the following discrete equation can be considered to calculate the distance property ( $d$ ) of each grid point

$$d_{q+1} = d_q + v_q \Delta t; \quad q \in 0, 1, \dots, N \quad (3)$$

where  $\Delta t$  is the time step. Consider that  $\mathcal{K}$  is a set that contains all the possible paths that connect the starting point ( $p_0$ ) to the endpoint ( $p_N$ ). Furthermore, a vector of all maximum loads for the engines currently running is denoted  $\mathbf{p}^c$ . The total power at each grid point can be estimated as follows

$$P_{total}(v_q, d_q) = P_{prop}(v_q, d_q) + P_{hotel}(d_q) + P_{aux}(d_q); \quad q \in 0, 1, \dots, N. \quad (4)$$

As the path is predefined, the distance  $d_q$  from the starting point  $p_0$  will uniquely define the current position. The corresponding load level will be calculated as

$$\mathcal{L}(v_q, d_q) = \frac{P_{total}(v_q, d_q)}{\sum(\mathbf{p}^c)}; \quad q \in 0, 1, \dots, N. \quad (5)$$

Normally, all engines are run on the same load, and this is assumed here as well.

Considering  $\mathcal{F}(\cdot) : \mathbb{R} \rightarrow \mathbb{R}$  being a mapping (essentially based on Fig. 9, that shows specific fuel consumption for one engine) that takes the total power consumption and returns the fuel consumption, then

$$\mathbf{f}(v_q, d_q) = \mathcal{F}(P_{total}(v_q, d_q)); \quad q \in 0, 1, \dots, N \quad (6)$$

If switching between engine combinations is possible during the voyage, each relevant engine combination should one layer each as shown

in Fig. 8. By introducing  $F_{on}$  and  $F_{off}$ , which are on/off switching penalties, the optimization problem can be defined as

$$\mathbf{v}_{ship}^o = \arg \min_{v_k \in \mathcal{V}} \left( \sum_{k \in \mathcal{K}} f(v_k, d_k) + n_{on} F_{on} + n_{off} F_{off} \right) \quad (7)$$

subject to Eqs. (3), (4), and where  $n_{on}$  and  $n_{off}$  show the number of engines turning on and off respectively during the voyage.

To solve this optimization problem, a unidirectional graph is introduced. The nodes in this graph are defined by the relevant attributes, encompassing local/global time, distance from the initial point, geographical coordinates, weather data, average hotel power consumption, and engine configuration. The edges connecting these nodes carry weights that symbolize fuel consumption during node transitions. This graph can be used to minimize fuel consumption using dynamic programming. The attributes stored in the nodes are employed to predict hotel and auxiliary power demand, as computed in the preceding section. Propulsion power is predicted using the NAPA API. Consequently, this propulsion power prediction is integrated into an auxiliary model. This integrated model allows us to predict the total power required for the cruise ship.

To accurately predict fuel consumption for each edge, it is crucial to consider the Specific Fuel Consumption (SFC) of the ship's engines, as shown in Fig. 9. SFC measures engine efficiency by quantifying the fuel required to generate a unit of power. Lower SFC values indicate higher engine efficiency. Distinct SFC curves shown in Fig. 9 are utilized to enhance conventional versus next-generation engine comparison. As depicted in Fig. 9, conventional engines are optimal at 85% load, while newer engines, with lower SFC, are efficient at 100%. Below is information on both engine types.

*Conventional engine:* The selected four-stroke engine has the most efficient fuel economy at the time of construction of the ship. It also has good power-to-weight and power-to-space ratios and adheres to the IMO Tier II exhaust emissions regulations. Marine Diesel Oil (MDO) or Light Fuel Oil (LFO) are acceptable fuels.

*Next-generation engine:* The selected four-stroke engine introduces versatility through its dual-fuel capability. This engine transitions between gas and diesel operating modes, ensuring uninterrupted power generation. Primarily optimized for superior fuel economy, it offers ultra-low emissions when operating on gas, with nearly all NOx emissions effectively mitigated. Compatible fuels include natural gas, LFO, and Liquid Biofuel (LBF). When running on gas, it adheres to IMO III emissions standards. This engine type exhibits a 25% weight reduction and a 12% decrease in length compared to the conventional one with the same power output.

The above describe speed optimization method is tested on two scenarios. In the first scenario, the voyage duration is fixed at the value of 32 h, which is equal to the actual duration. In the second scenario, the voyage duration varies from 30 to 34 h. An hourly time step is considered for all simulations. The ship has four engines: two small (denoted as  $S$ ) and two large (denoted as  $L$ ). It is worth noting that, on the sea, one avoids using only one engine and all four engines, but all other five combinations are considered in this study:  $C = \{SS, LS, LL, LSS, LLS\}$ . The admissible ship speed is considered to be  $\mathcal{V} = \{v_{avg} + \Delta v \cdot k, k = -4, -3, \dots, 3, 4\}$ , where  $v_{avg} = (\text{total distance}) \times (\text{total duration})^{-1}$ , and  $\Delta v$  is chosen to be  $1 \text{ km h}^{-1}$ . The speed used in the measurement case is used to build the path related to the base case; see Fig. 10. It can be seen that in the middle of the voyage, the ship operators decided to increase the speed of the ship to guarantee the arrival time.

#### 3.1. Fix voyage duration

In this section, a 32-h voyage is analyzed, conducting two observations. Initially, the impact of optimal speed on fuel consumption is investigated. Subsequently, the effect of the speed profile optimization

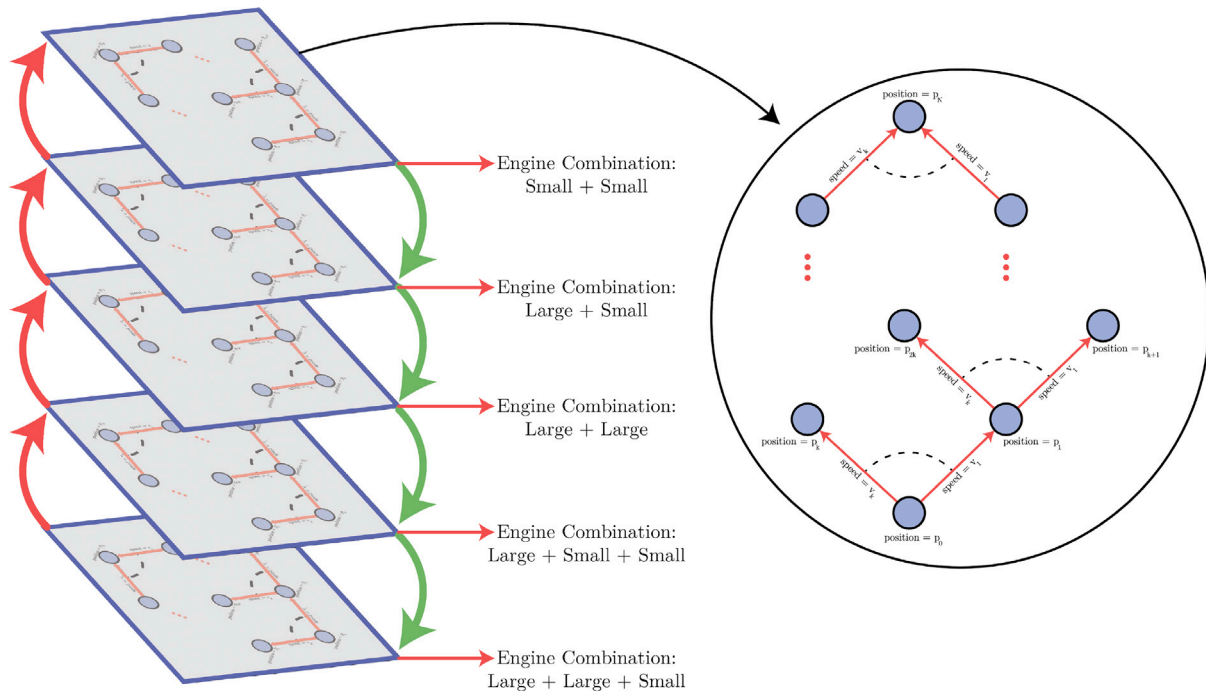


Fig. 8. A unidirectional graph showcasing five layers of engine combinations for optimization of power use during a voyage. Note that traveling from each layer to each other layer is possible.

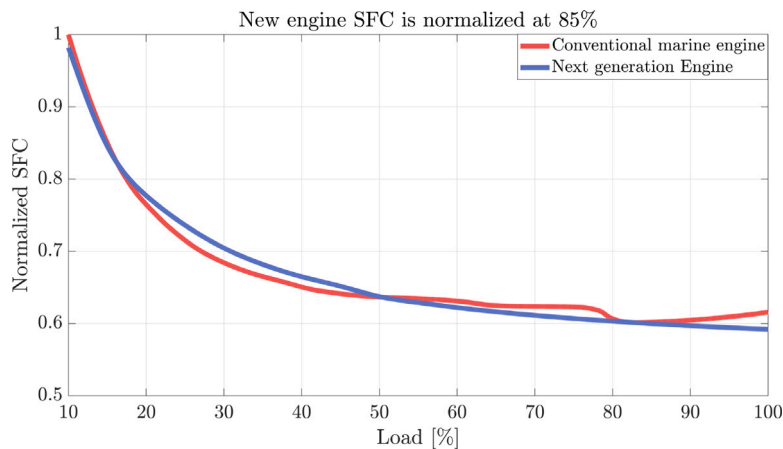


Fig. 9. Comparison of Specific Fuel Consumption (SFC) between conventional and next-generation engines. The SFC curve for the next-generation engine is normalized against the conventional engine’s SFC curve at 85% load.

on the fuel consumption performance of next-generation and conventional engines is compared. Simulations, using nowcasts of actual weather, are conducted at load levels of 85% and 100% for both engine types. Results in Table 4 show that the next-generation engines yield a 2.74% fuel saving compared to the measured data. Moreover, it is feasible to replace two large and one small engine with one large and two small engines for the voyage. Further insights on load levels and (SFC) are presented in Fig. 11, indicating that next-generation engines perform optimally at a load level close to 100%, aligning with expectations from Fig. 9.

The graph related to the speed profile optimization can be seen in Fig. 12-(c), -(f), -(i), and -(l). The engine combinations used during the voyage can be seen in these figures. It can be observed that there are nine edges between each node, which correspond to nine different speed options. To facilitate examination, the graph illustrating all five graphs related to different engine combinations has been color-coded. For instance, it can be seen in Fig. 12-(i) that using the next-generation engine at 100% maximum load level, the *LSS* combination is used for

one hour.

Considering Fig. 11-(a), in some parts of the voyage, the engines are not working at the optimal load level. In future studies, the engines can be enforced to operate at the efficient load level, which is 85% for conventional engines and 100% for next-generation engines, and the surplus power can be stored in battery packs and utilized instead of fuel in certain situations.

### 3.2. Variable voyage duration

In this section, the effect of voyage duration is carried out on the fuel consumption. According to Table 5, it can be seen that the voyage duration is considered to be 30, 31, 32, 33, and 34 h for both conventional and next-generation engine models. Here, the maximum allowable load for conventional and next-generation engines is considered 85% and 100%, respectively. It can be observed that by extending the voyage duration by 2 h, a 6.08% fuel saving is achieved for the

**Table 4**  
Simulation results regarding fixed voyage duration.

	Engine model	Max power	Total fuel consumption (ton)	Fuel saving (%)	Constant speed load level (%)	Deviation from efficient load level (%)	Engine combination
Measurement	Conventional	85%	139.5	–	79.1	5.9	LL, LLS
	Next generation	100%	137.2	–	79.1	20.9	LL, LLS
Optimal	Conventional	85%	134.87	3.32	82.8	2.2	LL, LS
		100%	134.75	3.40	84.47	0.53	LL, LS
	Next generation	85%	133.5	2.70	80.98	4.02	LSS, LS
		100%	133.44	2.74	96.16	3.84	LSS, LS

**Table 5**  
Results of variable voyage duration simulations. In this table, opt stands for optimal, and cte stands for constant.

Engine model	Voyage duration (h)	Engine combination (optimal)	Engine combination (average)	Opt vs. actual fuel saving (%)	Opt vs. cte speed fuel saving (%)	Average load level (%)
Conventional	30	LSS, LL	LLS, LSS	–1.30	0.98	82.51
	31	LSS, LL	LLS, LSS, LL	1.44	1.62	82.94
	32	LL, LS	LLS, LL	3.32	1.29	82.74
	33	LL, LS	LLS, LL	4.78	2.27	82.73
	34	LL, LS	LL, LS	6.08	2.04	82.91
Next-generation	30	LL, LS	LL	–1.26	0.36	96.71
	31	LL, LS	LL, LS	0.97	0.49	94.77
	32	LSS, LS	LL, LS	2.74	0.09	96.16
	33	LS	LL, LS	4.22	0.18	92.56
	34	LS, SS	LS	5.41	0.15	93.12

**Table 6**  
Key features and their significance in hotel and auxiliary power modeling.

Features	Impact on predicted power usage (%)	
	Feature increased 5%	Feature increased 10%
$T_{amb}$	0.45%	0.87%
$H_{amb}$	0.14%	0.27%
$T_{sea}$	0.003%	–0.0003%
$V_{wind}$	0.05%	0.09%
$P_{amb}$	–0.03%	–0.06%
$P_{hotel,avg}$	1.47%	2.89%
$P_{prop}^a$	0.43%	1.61%

<sup>a</sup> Does only contain the indirect influence through the auxiliary power, not the direct propulsion power.

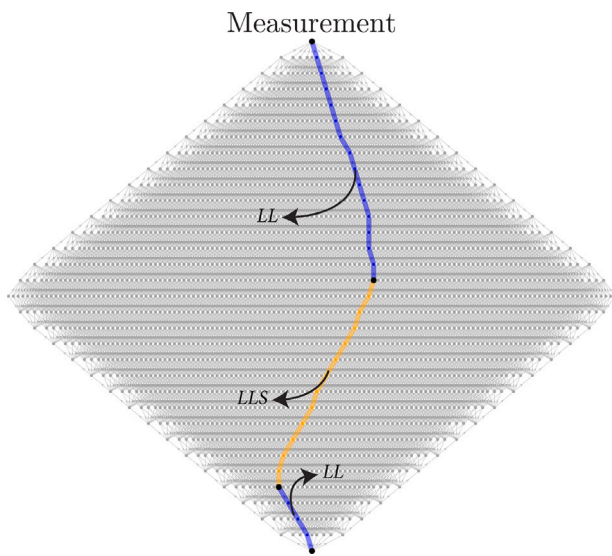


Fig. 10. Speed profile used in the measurement case.

conventional type and a 5.41% fuel saving for the next-generation type. All the speed profiles are depicted in Fig. 12, which also shows the engine combinations used in the voyage. In Table 5, a constant speed case is considered, representing a case in which the ship’s speed is constant and equal to  $v_{avg}$ .

### 3.3. Sensitivity analysis and impact of environmental factors

In order to get a picture how sensitive the results are to the predictions of the different features used in the model, Table 6 present how much the hotel and auxiliary energy demand changes if a feature is changed from its mean value by 5 or 10% of its range in the studied 32 h test journey. Most surprising result is the impact on the sea temperature. The hotel load model predicts increased power demand if the sea temperature increases, while the auxiliary model predicts lower power demand; together the effects are close to zero.

These power demands were not transformed into fuel consumption, as that would require using a certain SFC curve. That would make the results depend where we happen to be on the SFC curve, which would increase the randomness of the results. The main result can anyway be read from Table 6, model prediction uncertainty based on the other variables except  $P_{hotel,avg}$  and  $P_{prop}$  are pretty small. Propulsion power has by far the largest influence, as it is about twice as large as hotel and auxiliary power together. Any system using the suggested speed optimization should probably track changes in required propulsion load and average hotel load in order to be successful in the long run.

### 3.4. Real-time application in cruise operations

Incorporating the proposed optimization framework into real-time cruise operations could significantly enhance modern vessels’ operational efficiency. The framework can dynamically adjust ship speed throughout a voyage by using existing onboard energy management systems and real-time data inputs, such as weather forecasts and engine performance metrics. This section discusses how real-time data acquisition, adaptive optimization, and automated decision support can facilitate the continuous refinement of the optimization process, ensuring optimal fuel efficiency under changing environmental and operational conditions. To effectively implement the proposed method in real-time cruise operations, the following five key factors are discussed:

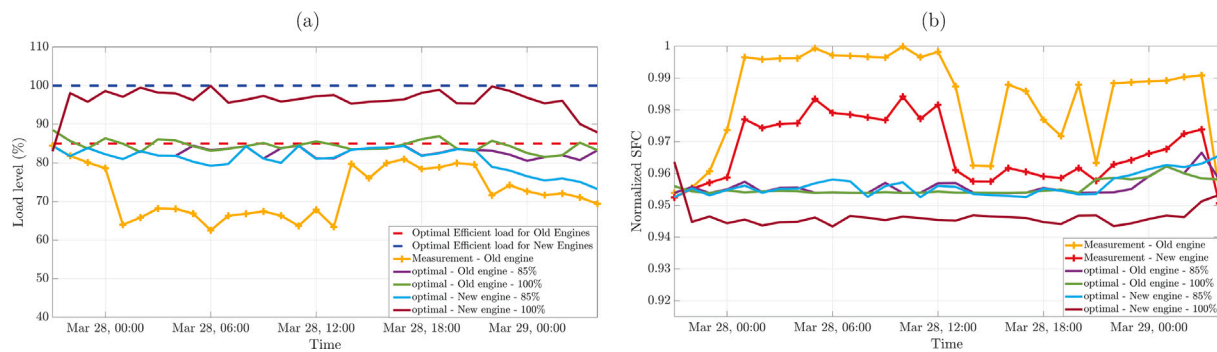


Fig. 11. Load level and normalized SFC in the fixed voyage duration case.

- **Integration with Onboard Systems:** The proposed optimization method can be seamlessly integrated into modern cruise ships' energy management and navigation systems. These systems can interface with external data sources, such as weather forecasts and voyage planning tools (e.g., NAPA). By using this infrastructure, the optimization algorithm can dynamically receive real-time updates on environmental conditions (e.g., wind speed, sea state, currents) and ship performance (e.g., engine load, fuel consumption), allowing continuous and real-time adjustments.
- **Real-Time Data Acquisition:** The critical inputs for real-time optimization, such as propulsion power demand, weather data, hotel, and auxiliary loads, can be gathered continuously from onboard sensors and external data providers. This data stream enables real-time recalibration of the models as conditions change during the voyage. Additionally, integration with external weather services (such as those used by NAPA) ensures that speed and engine size adjustments remain responsive to environmental conditions.
- **Automated Decision Support:** In practical use, the optimization method can serve as a decision-support tool for the crew, generating optimal speed and engine configuration recommendations. The crew can review and manually implement these suggestions, or the system could evolve to automatically adjust engine settings and speed within pre-defined safety and operational constraints, thus enhancing overall efficiency.
- **Hybrid Control Systems:** As the maritime industry transitions towards hybrid propulsion systems incorporating battery storage and alternative fuels, our method can be further extended to optimize power distribution among different energy sources in real-time. This would ensure that all available energy sources are utilized at maximum efficiency, making the system particularly useful for future ships with hybrid configurations.

### 3.5. Scalability and adaptability to different ship types

While validated on a specific cruise ship case, the proposed optimization framework is designed to be flexible and scalable for other ship types and propulsion systems. The core modeling techniques, including regression models and neural networks, are adaptable to various operational profiles by re-training the models with new data specific to different vessels.

The NAPA API, used for propulsion power calculation, can be reconfigured to incorporate the hydrodynamic properties of various ship types, ensuring accurate power estimation across different vessel configurations. This makes the method adaptable for vessels with different propulsion systems, such as hybrid, LNG, or electric propulsion. In cases where such APIs are not available, there is a wealth of literature offering methods for modeling propulsion power (Solonen et al., 2023; dos Santos Ferreira et al., 2022; Lang et al., 2022; van Dooren et al., 2023).

## 4. Engine size optimization

Choosing the engine size of a ship optimally can yield significant advantages across multiple fronts. By selecting the most suitable engine size, a ship's system can operate more efficiently, reducing fuel consumption and lowering constructional/operational costs. Additionally, optimal engine sizing allows for the integration of propulsion systems that match the vessel's specific requirements, ensuring that power generation meets demand without unnecessary excess or strain on the engine components. This extends the engine's lifespan, reducing maintenance needs and associated costs. Overall, the strategic selection of engine size represents a critical decision point in ship design and construction, with far-reaching implications for operational performance and economic sustainability. The two different engine types studied so far are also considered here.

Genetic Algorithm (GA) is an optimization algorithm inspired by natural selection and genetics (Golberg, 1989). It belongs to evolutionary algorithms and is widely used on difficult non-convex problems across various domains.

Using the speed profile optimization developed in the last section and considering the engine topology the same as it was, the optimization problem (Eq. (7)) augmented by letting the maximum load  $p^c$  of each engine be an optimization variable.

These two criteria are considered in the optimization problem: (i) : The total power of the engines selected by the algorithm must be greater than or equal to the maximum power used by the captain in a month of measured data, (ii) : The power of two engines must be smaller or equal to the other two engines. Also, the available search space for all the engines is between 4 to 18 MW. The results of these two scenarios are reported in Table 7 and are discussed in detail in the following.

### 4.1. First scenario: two large engines of same sizes, and two small of same size

In conventional engines, a ship is equipped with two large engines, each capable of producing 13.9 MW, and two smaller engines, each rated at 4.2 MW. In the same 32-h voyage, two large engines and one small engine operate for the first three hours, followed by two large engines for the rest. This optimization results in a 3.40% fuel savings.

With next-generation engines, optimal sizing entails large engines of 11.8 MW and small engines of 4.3 MW. The engine combinations used during the voyage are the same as in the previous one. This setup yields a fuel saving of 4.81%. Adopting next-generation engines has significantly reduced engine size compared to the previous engine type.

### 4.2. Second scenario: two different large and two different small engines

In scenario 2, the optimal configuration for the conventional engine type includes two large engines with power capacities of 14.5 and 13

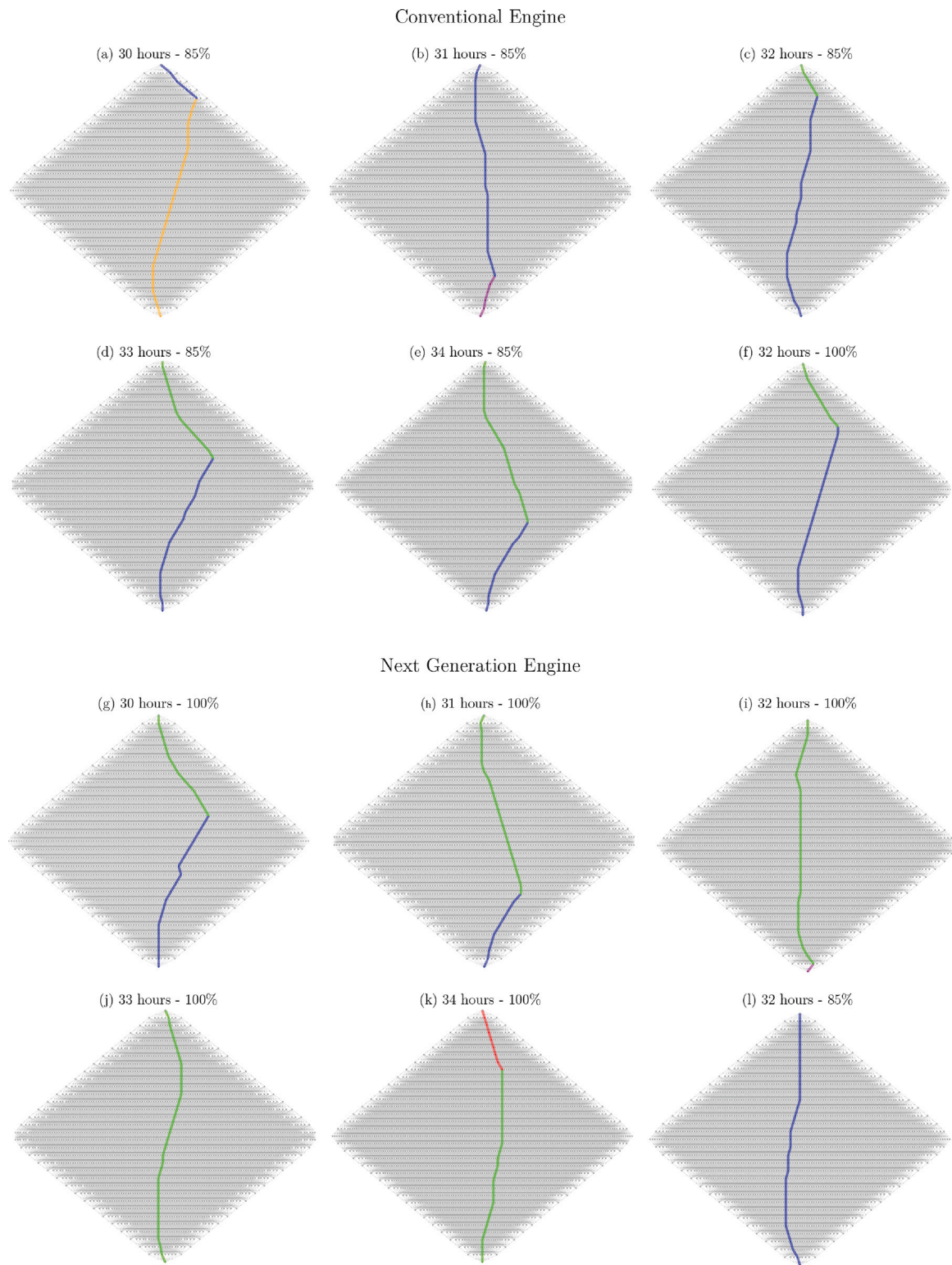


Fig. 12. The optimal speed profiles and engine combinations considered in the simulations. Regarding engine combinations, red is *SS*, green is *LS*, blue shows *LL*, purple indicates *LSS*, and yellow is *LLS*.

MW and two small engines with power capacities of 7.4 and 5.3 MW. This configuration will save fuel up to 3.44%. In the voyage, two large engines and one small engine operate for the first four hours, followed by two large engines for the rest.

For the next-generation engine, the algorithm finds optimal performance with two equally large engines with a capacity of 11.6 MW and two small engines with a capacity of 6 and 5 MW. The engine

combinations used during the voyage are the same as mentioned in the previous paragraph.

### 5. Conclusion

In conclusion, this paper presented a methodology that integrated data-based modeling techniques with a combination of optimization

**Table 7**  
Optimal engine sizes and associated fuel savings.

Scenario	Engine type	Engine 1	Engine 2	Engine 3	Engine 4	Fuel saving (%)
1	Conventional	13.9	4.2	13.9	4.2	3.40
	Next-generation	11.8	4.3	11.8	4.3	3.21
2	Conventional	14.5	7.4	13	5.3	3.44
	Next-generation	11.6	6	11.6	5	3.22

of the engine configuration and the speed of the ship. A method using dynamic programming for minimization fuel consumption while keeping time table was presented and utilized. The method used the NAPA Voyage Optimization API to provide information about how the ship requires propulsion power for keeping a certain speed at the weather conditions at hand. Passenger-induced hotel load and other non-propulsion auxiliary load were predicted using a machine learning model obtained from ship data. The proposed method showed in a test case fuel savings of up to 3.3% with conventional engines and 2.7% with next-generation engines. Furthermore, optimizing engine size contributed to an additional 0.5% reduction in the fuel consumption.

While the proposed methodology offers promising results, certain limitations should be acknowledged. The study was made using data from a single cruise ship, and no guarantees for that the method generalizes to other ships are given. The optimization framework uses predictions of environmental conditions, and actual weather or sea state fluctuations could affect the expected fuel savings. Additionally, variability in passenger load could influence hotel power consumption, leading to deviations in the predicted fuel efficiency.

It should however be noted, that almost as good results could have been obtained using simpler methods. The main gains comes from prediction of the hotel load, which could be predicted to a quite high enough accuracy using the hourly average curve, and distribution of the speed according to that and the known SFC curves of the engines. This information is easily available for any cruise ship. The sensitivity analysis in Section 3.3 also implies that the impact on environmental conditions seem be to quite small, so the impact of the change of speed can most likely be estimated quite well using just the basic formula that the power demand is proportional to the cube of the speed. This would introduce an autoregressive feature to the model, which is missing from the current model, and which is often good for prediction. Thus, pretty good results could most likely be obtained by predicting the hotel load by using the hourly averages, and by assuming that the current propulsion power will change proportionally to the cube of the speed. And the auxiliary power does mainly vary with the total power. This all would result in an extremely simple prediction model, that would be available on any ship, in particularly if no voyage optimization software is available. And the model would be more only be based on data, and possibly have no parameters, which would make it extremely simple to transfer between ships. There is also an element of feedback involved, as the speed optimization suggests a certain speed, not a certain propulsion power. And one could add one more layer of feedback correction, if the change of speed results in a different propulsion load change than the predicted one, the speed change can be corrected towards the predicted one. Thus, the sensitivity of the speed optimization on the prediction of the propulsion loads might not be that high at all. This all will be investigated in the near future.

Regarding other future work, the validation of the method on other ships is a clear next step. The integration of energy storage systems and the development of real-time adaptive algorithms for dynamic power management represent promising avenues for future research. Additionally, implementing online modeling and optimization techniques enables continuous refinement of propulsion system efficiency in real-world operating conditions.

## CRediT authorship contribution statement

**Arash Marashian:** Writing – original draft, Visualization, Software, Formal analysis, Data curation. **Jari M. Böling:** Writing – review & editing, Supervision, Project administration, Methodology, Conceptualization. **Abolhassan Razminia:** Writing – review & editing, Supervision, Methodology, Formal analysis. **Jari Hyvönen:** Resources, Conceptualization. **Roberto Vettor:** Writing – review & editing, Resources, Methodology. **Wilhelm Gustafsson:** Resources. **Mathias Pirttikangas:** Resources. **Jerker Björkqvist:** Supervision.

## Declaration of competing interest

The authors declare the following financial interests/personal relationships which may be considered as potential competing interests: Arash Marashian reports financial support was provided by Business Finland. Abolhassan Razminia reports financial support was provided by Business Finland. If there are other authors, they declare that they have no known competing financial interests or personal relationships that could have appeared to influence the work reported in this paper.

## Acknowledgments

Financial support from the Business Finland projects CPT (40323/31/2020) and INDECS (7682/31/2022) are gratefully acknowledged.

## References

- Baldi, F., Ahlgren, F., Nguyen, T.-V., Thern, M., Andersson, K., 2018. Energy and exergy analysis of a cruise ship. *Energies* 11 (10), 2508.
- Balsamo, F., Capasso, C., Lauria, D., Veneri, O., 2020. Optimal design and energy management of hybrid storage systems for marine propulsion applications. *Appl. Energy* 278, 115629.
- Bouman, E.A., Lindstad, E., Riialand, A.I., Strømman, A.H., 2017. State-of-the-art technologies, measures, and potential for reducing GHG emissions from shipping—A review. *Transp. Res. D* 52, 408–421.
- Brækken, A., 2021. Energy Use and Energy Efficiency Potential on Passenger Ships (Master's thesis). NTNU, Trondheim, Norway.
- Cheliotis, M., Lazakis, I., Theotokatos, G., 2020. Machine learning and data-driven fault detection for ship systems operations. *Ocean Eng.* 216, 107968.
- dos Santos Ferreira, R., de Lima, J.V.P., Caprace, J.-D., 2022. Comparative analysis of machine learning prediction models of container ships propulsion power. *Ocean Eng.* 255, 111439.
- 2024. European commission. [https://climate.ec.europa.eu/eu-action/transport/reducing-emissions-shiping-sector\\_en](https://climate.ec.europa.eu/eu-action/transport/reducing-emissions-shiping-sector_en). (Accessed 24 March 2024).
- Fan, A., Yang, J., Yang, L., Wu, D., Vladimir, N., 2022. A review of ship fuel consumption models. *Ocean Eng.* 264, 112405.
- Fang, S., Xu, Y., Wen, S., Zhao, T., Wang, H., Liu, L., 2019. Data-driven robust coordination of generation and demand-side in photovoltaic integrated all-electric ship microgrids. *IEEE Trans. Power Syst.* 35 (3), 1783–1795.
- Golberg, D.E., 1989. *Genetic Algorithms in Search, Optimization, and Machine Learning*. Addison-Wesley.
- Hansen, J.F., Wendt, F., 2015. History and state of the art in commercial electric ship propulsion, integrated power systems, and future trends. *Proc. IEEE* 103 (12), 2229–2242.
- Huotari, J., Manderbacka, T., Ritari, A., Tammi, K., 2021. Convex optimisation model for ship speed profile: Optimisation under fixed schedule. *J. Mar. Sci. Eng.* 9 (7), 730.
- 2024. International Maritime Organization (IMO). <https://www.imo.org/en/MediaCentre/HotTopics/Pages/Cutting-GHG-emissions.aspx>. (Accessed 24 March 2024).
- Kim, H., Koo, K.Y., Joung, T.-H., 2020. A study on the necessity of integrated evaluation of alternative marine fuels. *J. Int. Marit. Saf. Environ. Aff. Shipp.* 4 (2), 26–31.

- Lang, X., Wu, D., Mao, W., 2022. Comparison of supervised machine learning methods to predict ship propulsion power at sea. *Ocean Eng.* 245, 110387.
- Li, H., Xu, B., Lu, G., Du, C., Huang, N., 2021. Multi-objective optimization of PEM fuel cell by coupled significant variables recognition, surrogate models and a multi-objective genetic algorithm. *Energy Convers. Manage.* 236, 114063.
- Ma, D., Ma, W., Jin, S., Ma, X., 2020. Method for simultaneously optimizing ship route and speed with emission control areas. *Ocean Eng.* 202, 107170.
- Marashian, A., Razminia, A., 2024. Mobile robot's path-planning and path-tracking in static and dynamic environments: Dynamic programming approach. *Robot. Auton. Syst.* 172, 104592.
- Marashian, A., Razminia, A., Shiryaev, V.I., Ossareh, H.R., 2024a. Longitudinal model identification of multi-gear vehicles using an LPV approach. *Math. Comput. Simulation* 216, 1–14.
- Marashian, A., Waris, A., Razminia, A., Böling, J., Manderbacka, T., Vettor, R., Huotari, J., Gustafsson, W., Pirttikangas, M., Stigler, C., Björkqvist, J., Manngård, M., 2024b. Optimizing cruise ship speed incorporating weather and hotel load factors. In: 24th European Control Conference. ECC24.
- Micallef, A., Apap, M., Licari, J., Caruana, C., 2024. A two-stage approach combining constraint-based algorithms and Gaussian process regression for estimation of cruise ship hotel loads. In: 2024 IEEE 22nd Mediterranean Electrotechnical Conference. MELECON, IEEE, pp. 750–755.
2023. NAPA voyage optimization. <https://www.napa.fi/software-and-services/ship-operations/napa-fleet-intelligence/voyage-optimization/>. (Accessed 06 November 2023).
- Piispa, M.-P., 2020. Optimizing Fuel Consumption for a Sustainable Future, Seabourn Ovation - Fuel Economy of Sea Voyages 2019 (Master's thesis). Novia University of Applied Sciences, Turku, Finland.
- Psarafitis, H.N., Kontovas, C.A., 2014. Ship speed optimization: Concepts, models and combined speed-routing scenarios. *Transp. Res. C* 44, 52–69.
- Radonja, R., Pelić, V., Pavić, D., Glujić, D., 2019. Methodological approach on optimizing the speed of navigation to reduce fuel consumption and increase energy efficiency of the cruising ship. *Pomorstvo* 33 (2), 222–231.
- Simonsen, M., Walnum, H.J., Gössling, S., 2018. Model for estimation of fuel consumption of cruise ships. *Energies* 11 (5), 1059.
- Simorgh, A., Marashian, A., Razminia, A., 2019. Adaptive pid control design for longitudinal velocity control of autonomous vehicles. In: 2019 6th International Conference on Control, Instrumentation and Automation. ICCIA, IEEE, pp. 1–6.
- Simorgh, A., Razminia, A., Marashian, A., 2024. Adaptive velocity control of an autonomous vehicle using input–error model reference approach. *J. Franklin Inst.* 106700.
- Solonen, A., Maraia, R., Springer, S., Haario, H., Laine, M., Rätty, O., Jalkanen, J.-P., Antola, M., 2023. Hierarchical Bayesian propulsion power models—A simplified example with cruise ships. *Ocean Eng.* 285, 115226.
- Tadros, M., Ventura, M., Guedes Soares, C., 2023. Review of the decision support methods used in optimizing ship hulls towards improving energy efficiency. *J. Mar. Sci. Eng.* 11 (4), 835.
2024. Tidetechn. <https://www.tidetechn.org/>. (Accessed 27 May 2024).
- Tillig, F., Mao, W., Ringsberg, J., 2015. Systems Modelling for Energy-Efficient Shipping. Tech. Rep., Chalmers University of Technology.
- van Dooren, S., Dühr, P., Onder, C.H., 2023. Convex modelling for ship speed optimisation. *Ocean Eng.* 288, 115947.
2024. Wärtsilä engine online configurator. <https://www.wartsila.com/marine/engine-configurator>. (Accessed 25 March 2024).
- Yang, W., Wang, K., Zuo, W., 2012. Neighborhood component feature selection for high-dimensional data. *J. Comput.* 7 (1), 161–168.
- Zis, T.P.V., Psarafitis, H.N., Ding, L., 2020. Ship weather routing: A taxonomy and survey. *Ocean Eng.* 213, 107697.